HHS Public Access

Author manuscript

Adv Healthc Mater. Author manuscript; available in PMC 2021 August 01.

Published in final edited form as:

Adv Healthc Mater. 2020 August ; 9(15): e1901794. doi:10.1002/adhm.201901794.

Three Dimensional Bioprinting of Oxygenated Cell-Laden Gelatin Methacryloyl Constructs

Ahmet Erdem[1,2,3,4,#], **Mohammad Ali Darabi**[1,2,5,#], **Rohollah Nasiri**[1,2,6], **Sivakoti Sangabathuni**[1,2], **Yavuz Nuri Ertas**[2,7,8], **Halima Alem**[1,2,9], **Vahid Hosseini**[1,2,5], **Amir Shamloo**[6], **Ali S. Nasr**[10], **Samad Ahadian**[1,2,5], **Mehmet R. Dokmeci**[1,2,5,11], **Ali Khademhosseini**[1,2,5,11,12,*], **Nureddin Ashammakhi**[1,2,11,*]

[1]Center for Minimally Invasive Therapeutics (C-MIT), University of California, Los Angeles, California, USA

[2]Department of Bioengineering, University of California, Los Angeles, California, USA

[3]Department of Chemistry, Kocaeli University, Umuttepe Campus, 41380, Kocaeli, Turkey

[4]Department of Biomedical Engineering, Kocaeli University, Umuttepe Campus, 41380, Kocaeli, Turkey

[5]Terasaki Institute for Biomedical Innovation, Los Angeles, California, USA

[6]Department of Mechanical Engineering, Sharif University of Technology, Tehran, 11365-11155, Iran

[7]Department of Biomedical Engineering, Erciyes University, 38039, Kayseri/Turkey

[8]Nanotechnology Research Center (ERNAM), Erciyes University, 38039 Kayseri, Turkey

[9]Université de Lorraine, CNRS, IJL, F-54000 Nancy, France

[10]Division of Cardiothoracic Surgery, Department of Surgery, University of Iowa Hospitals and Clinics, Carver College of Medicine, University of Iowa, Iowa City, Iowa 52242, USA

[11]Department of Radiological Sciences, David Geffen School of Medicine, University of California, Los Angeles, California, USA

[12]Department of Chemical and Biomolecular Engineering, University of California, Los Angeles, California, USA

Abstract

[(*)]Corresponding authors California NanoSystems Institute (CNSI), University of California – Los Angeles, 570 Westwood Plaza, Building 114, Room 4523, Los Angeles CA 90095, USA, Tel. +1 310 794 5845, n.ashammakhi@ucla.edu, khademh@terasaki.org.

Author Information

Contributions

A.E. and M.A.D. designed the project, wrote the manuscript and conducted experiments. R.N. and S.K. wrote the manuscript and conducted experiments. Y.N.E. conducted statistics and revised the manuscript. V.H., H.A., A.S.N. M.R.D. and S.A. revised the manuscript. N.A. and A.K. designed the experiments, wrote, edited and corresponded this manuscript. All authors reviewed the manuscript.

[(#)]First authors

Additional Information

Competing interests

The authors declare no competing interests.

Cell survival during the early stages of transplantation and before new blood vessels formation is a major challenge in translational applications of three-dimensional (3D) bioprinted tissues. Supplementing oxygen (O_2) to transplanted cells via an O_2 generating source such as calcium peroxide (CPO) is an attractive approach to ensure cell viability. Calcium peroxide also produces calcium hydroxide which reduces the viscosity of bioinks, which is a limiting factor for bioprinting. Therefore, adapting this solution into 3D bioprinting is of significant challenge. In this study, we developed a gelatin methacryloyl (GelMA) bioink that was optimized in terms of pH and viscosity. The improved rheological properties led to the production of a robust bioink suitable for 3D bioprinting and controlled O_2 release. In addition, we characterized O_2 release, bioprinting conditions and mechanical performance of hydrogels having different CPO concentrations. As a proof of concept study, fibroblasts and cardiomyocytes were bioprinted using GelMA bioink containing CPO. Viability and metabolic activity of printed cells were checked after seven days of culture under hypoxic condition. The results showed that the addition of CPO improves the metabolic activity and viability of cells in bioprinted constructs under hypoxic condition.

Keywords

3D bioprinting; bioink; calcium peroxide; cardiomyocytes; hypoxia; oxygen

1. INTRODUCTION

Cell-based therapy has shown potential for tissue regeneration, but many attempts have failed to show the repopulation of damaged tissue due to poor survival of the transplanted cells [1, 2]. A major limitation for successful cell therapy can be attributed to hypoxia due to vascular injury [3]. For transplanted cells to survive, there should be sufficient nutrients and oxygen (O_2) supply. Cells can rely on diffusion of O_2 to a limited distance of ~ 200 microns [4]. Several days to weeks are needed for angiogenesis to develop *in vivo* [5], and during this critical time, most of transplanted cells will die while having no alternative supply of O_2. Thus, by providing O_2 to transplants, cells may survive through this critical period after delivery [6], leading to improved regeneration capacity. Furthermore, in conditions such as myocardial infarction (MI), loss of cardiomyocytes occurs due to the lack of blood supply. In such situation, externally delivered O_2 may also help vulnerable endogenous cardiomyocytes to withstand the harsh post-MI hypoxic conditions [7]. It was found that O_2 release is associated with increased angiogenesis in the heart in post-MI period in rats, which is probably due to enhanced survival of endothelial cells [8].

Recently, O_2 generating biomaterials have gained attention. Various O_2 materials have been explored as source of O_2, including sodium percarbonate ($(Na_2CO_3)_2.3H_2O_2$) [9], calcium peroxide (CPO) [10], magnesium peroxide and hydrogen peroxide (H_2O_2) [8, 11]. Among these sources, CPO was found to be one of the best peroxides to provide prolonged O_2 release, without needing encapsulation, and it has been thus used more frequently in O_2 generating biomaterials [6]. CPO dissociates first to H_2O_2 and $Ca(OH)_2$, which increases the pH in the O_2 generating biomaterial. Then, H_2O_2 is converted to water and O_2. Oxygen release kinetics from peroxide compounds is influenced by different factors such as temperature [12], pH [13], and the use of catalase [13, 14]. To reduce the risk of the

generation of hydroxyl free radicals, a catalase is being used in the preparation of O_2 releasing biomaterials. The use of higher concentrations of O_2 can be toxic to cells [15]. Alemdar *et al.* tested CPO with cardiomyocyte-laden gelatin methacryloyl (GelMA) discs (prepared by using two glass slides) *in vitro,* and they found that cells survival and proliferation were enhanced for over five days [16, 17].

Three-dimensional bioprinting has been increasingly recognized as an advanced technology that can address many problems seen with conventional methods of tissue engineering, especially engineered tissue survival, integration and angiogenesis [18]. It is known that 3D bioprinting can be used for producing personalized therapeutic patches by using patient specific biologics. Robust 3D bioprinted constructs can further be used with the use of minimally invasive procedures [19, 20]. In a combinatorial approach, cell and an O_2 source-containing bioinks can be used to fabricate patches using 3D bioprinting. It was therefore, envisioned that developing such an approach can help loaded cells and possibly compromised cells in the injured area, which can be of great benefit in future. GelMA has been investigated extensively for various tissue bioprinting applications, and it was found to enhance cellular adhesion [21, 22], and it was selected as bioink biomaterial of choice in our study. It is hypothesized that by supplying O_2 in the bioink, cell survival and function during and after the process of bioprinting can be improved which can also be reflected on the subsequent function of the resulting 3D printed constructs.

In this study, O_2 releasing 3D bioprinted constructs were developed by the addition of CPO as an O_2 source to the GelMA bioinks. One of the important parameters that should be considered in extrusion-based 3D bioprinting is the viscosity of the bioinks. It is known that viscosity affects both printing quality and processing as well as cell viability. We discovered that using CPO in 3D bioprinting demands a trade-off between amount of CPO being used, pH of the solution, and viscosity of bioink. The use of CPO as an O_2 source leads to the release of $Ca(OH)_2$ ions which affects the viscosity of bioink by the changing pH. The elimination of CPO side effect in the bioink composition was achieved using a buffer solution. Therefore, O_2 releasing bioink reported in the current study may change the paradigm in engineering and application of tissue constructs in 3D modelling and for regenerative therapy.

2. MATERIALS AND METHODS

Gelatin (Type A, 300 bloom from porcine skin), methacrylic anhydride (MA), calcium peroxide (CPO), catalase (obtained from bovine liver, 2000 – 5000 units mg^{-1} protein), 2-hydroxy-4’-(2-hydroxyethoxy)-2-methyl propiophenone (photoinitiator, PI), phosphate-buffered saline (PBS) and Alizarin red S were obtained from Sigma-Aldrich (St. Louis, MO, USA). Dulbecco’s phosphate buffered saline (DPBS), trypsin-EDTA, and penicillin −streptomycin were purchased from Fisher Scientific. Alpha-modified Eagle’s medium (Gibco 11965–092, Invitrogen Co., USA was supplied by Invitrogen (Grand Island, NY, USA). FBS and precleaned microscope slides were obtained from Fisher Scientific (Waltham, MA, USA). The live/dead viability/cytotoxicity kit was obtained from Invitrogen (Grand Island, NY, USA). All reagents were used without further purification.

2.1. Gelatin Methacryloyl (GelMA) Synthesis

GelMA synthesis was performed using an earlier described technique [23]. Briefly, 10 g of porcine skin gelatin was completely dissolved at 60 °C in 100 mL of PBS for 60 min. Then, 8 mL of MA was added drop by drop to the gelatin mixture and permitted to react at 50 °C for 3 h. The blend was mixed with double volume of distilled water to prevent the reaction. The GelMA solution was dialyzed with 12–14 kDa dialysis tube for one week against distilled water. Then, the dialyzed product was freeze-dried and preserved for further use at −80 °C.

2.2. Preparation of the O_2 Releasing Bioink

For the preparation of O_2 releasing bioink (CPO containing GelMA solution), three different stock solutions were prepared. In the first place, 10 mg of PI was dissolved in 1 mL of 0.1M HEPES buffer solution in order to gain a solid content with 1% (w/v) concentration. Then, 200 mg GelMA foam was added to this solution to get 20% (w/v) GelMA stock solution. For the 2% CPO stock solution, 48 °L hydrochloric acid (HCl, 37%) was added to 1mL of 0.1 M HEPES, before the addition of 20mg CPO. These two stock solutions were used with third stock solution (0.1 M HEPES) with different ratios to obtain 10% GelMA, 0.5% PI and different CPO containing oxygenated bioinks (Table 1).

2.3. Three-Dimensional Bioprinting

Four bioink groups were produced, containing 10% GelMA with 0%, 0.1%, 0.5% and 1% CPO (Fig. 1A). In addition, 5×10^6 mL^{-1} of 3T3 fibroblast (NIH 3T3) cells (ATCC, Manassas, Virginia, USA) or 8×10^6 mL^{-1} of rat derived cardiomyocytes were added into bioinks. For cardiomyocyte isolation and suspension, we used a protocol published by our team earlier [24]. In brief, the heart of 1–2 day old neonatal Sprague-Dawley rats (Charles River, USA) was isolated and suspended in Ca2+,Mg2+ free Hank's balanced salt solution (HBSS, Gibco). The aorta and vena cava sections were then removed from the hearts. Subsequently, the hearts were cut into quarters and rinsed twice in cold HBSS. The heart pieces were then digested in a solution of 0.06% (w/v) trypsin (Sigma-Aldrich) in HBSS overnight (4°C). The tissues were then digested in collagenase II (200 U mL^{-1}, Worthington Biochemical Corp., USA) in HBSS (37°C) in five supplementary digestions of 4–8 min. Following digestion, cells were pre-plated for 45 min and non-adherent cells were collected for use as the rat cardiomyocyte population. Rat cardiomyocytes were cultured in Dulbecco's modified Eagle's medium (Gibco) containing glucose (4.5 g L^{-1}), 10% (v/v) fetal bovine serum (FBS, Gibco), 1% (v/v) HEPES (100 U mL^{-1}, Gibco), and 1% (v/v) penicillin-streptomycin (100 mg mL^{-1}, Gibco).

A commercial 3D bioprinter (Cellink BioX 3D BioPrinter, Cellink AB, Gothenburg, Sweden) was used to print constructs, employing 23G needle, 80 kPa pressure, 20 mm s^{-1} speed, while the substrate temperature was kept at 4 °C. Before printing, the 3D bioprinter chamber was sterilized using ultraviolet (UV) irradiation for 10 min. After printing, printed constructs were moved into UV chamber to crosslink by applying UV irradiation (Omnicure S2000, Excelitas Technologies, Salem, MA, USA) with 4 W cm^{-2} intensity for 40 s [25]. Light irradiation was applied at a distance of 8 cm from samples. Printability of each bioink

type was evaluated according to the filament spreading ratio, which was calculated by dividing the width of the printed filament by the needle diameter (23G needle: 337 μm) [26].

2.4. Characterization of Morphology and Morphological Changes

2.4.1 Scanning electron microscopy (SEM)—The microstructure of 3D printed GelMA hydrogels having different CPO concentrations was characterized by using scanning electron microscopy (SEM, Gemini column Zeiss Supra 40VP Field Emission Scanning Electron Microscope). To prepare samples for SEM, hydrogels without cells were UV cross-linked, kept in −80 ºC for 3 h, freeze-dried overnight and iridium coated. Microstructure and porosity of the hydrogels were analysed using the nearest distances plugin from ImageJ software and SEM images which were recorded using the SEM equipment. Also, energy disperse X-ray (EDX) spectroscopy was used to determine different element in the hydrogels .

2.4.2 Swelling of O_2 releasing bioinks—For each bioink type, the swelling ratio of three samples (8mm diameter and 1.5mm thickness) was determined. Acellular hydrogels were weighed and placed into DPBS solution and kept at 37 °C for 24h. The weight of swollen hydrogels was defined after removing excess water from the surface. The swelling ratio of hydrogels was calculated according to the formula: $(W_t - W_0)/W_{0;}$ where, W_t and W_0 represent the weight values of fully swollen and blot-dried hydrogels, respectively.

2.5 Mechanical Characterisation

2.5.1 Rheological behaviour—Rheological studies were performed using MCR-302 rheometer (Anton Paar Ltd., Graz, Austria) with a 25 mm diameter parallel plate geometry with a gap distance of 0.5 mm, for bioinks, and an 8 mm diameter parallel plate geometry with a gap distance of 1.0 mm for hydrogels. A solvent trap was used to prevent dehydration. The temperature dependence of G' and G" was obtained using temperature sweep (oscillation) by decreasing the temperature from 24 °C to 4 °C at a cooling rate of 1 °C min^{-1}. Then, the viscosity of bioinks was recorded at 4 °C from 0.1 to 100 shear rate.

2.5.2. Semi-Quantification of Bioink Printability—Printing quantification was performed following the procedure described by Liliang *et al.* [27], who introduced printability parameter (Pr), intended to quantify similarity with the nature of square-formed prints. This calculation was based on the circularity of enclosed area which is defined as $C= 4\pi AL^{-2}$ in where L is perimeter and A represents area. The highest circularity is at the C = 1 condition. When the C value is closer to the 1, the shape is close to the circle. The circularity for squared shapes is equal to $\alpha/4$ rather than circles and the Pr defined as $Pr= \pi C^{-1}/4 = L^2A^{-1}/16$. According to this equation, for an optimal printability, obtained Pr must be 1, when the connected channel forms a complete square shape at ideal viscosity of bioink. While higher Pr is obtained with the higher viscosity, the lower Pr is obtained with lower viscosity. In the Image-J program, optical images of printed constructs were analyzed in order to determine the perimeter and region of the interconnected channels to calculate the Pr of each printed construct (n= 3).

2.5.3 Compression—The mechanical properties of O_2 releasing hydrogels were tested using unconfined compressive test. The bioinks having different CPO concentrations were casted in PDMS molds (8mm diameter and 1 mm height) and exposed to the UV light (4 W cm^{-2}) for 40 s for crosslinking. The compression strength of hydrogels was evaluated at a cross speed of 0.5 mm s^{-1} and up to 60% strain, using a mechanical testing machine (Instron Model 5542, Norwood, MA, USA). The Young's modulus was determined based on the slope of the initial linear region, corresponding to 10% strain.

2.6. Oxygen Release Kinetics

To determine O_2 release kinetics from the hydrogels, samples having varying CPO content were separately placed in wells of a 12-well plate, each containing 1.5mL media and catalase (100 u mL^{-1}). Released O_2 in the media was measured using O_2-sensitive electrode (World Precision Instruments, ISO-OXY meter, TBR 1025 free-radical analyser, Sarasota, Fl, USA) while having hydrogels under hypoxic condition (1% O_2, 5% CO_2 and 94% N_2 incubator at 37 °C). Oxygen release was monitored daily for seven days.

2.7. Biological Assessment

To investigate the effect of having O_2 in 3D bioprinted constructs, NIH 3T3 fibroblasts-laden were used in bioinks having CPO in different concentrations ranging from 0.1% to 1% and cultured for 7 days in hypoxic conditions.

2.7.1. In vitro cell culture—Fibroblasts were cultured in T175 flasks with Dulbecco's modified eagle's medium containing 10% bovine serum and 1% penicillin-streptomycin (Pen Strep, Pen Strep 15140, Fisher Scientific, Waltham, MA, USA). Trypsin (0.5%) was used to remove adherent cells from the surface of Petri dish. During the experiments, 100 u mL^{-1} catalase was added into the media (1.5 mL per well) while performing the experiments. Cell-laden CPO-GelMA bioinks were incubated in either normoxic (21% O_2, 5% CO_2 and 74% N_2) or hypoxic (1% O_2, 5% CO_2 and 94% N_2) condition for seven days.

2.7.2. Cell viability—To further understand the effect of O_2 release, live/dead assay (Invitrogen, Carlsbad, CA, USA) was performed for NIH 3T3 fibroblasts and cardiomyocytes in the 3D printed constructs having CPO microparticles in different concentrations and incubated under hypoxic condition. Constructs having no CPO microparticles and constructs kept in normoxic condition were used as controls. Before adding live/dead reagents, constructs were washed three times with DPBS. Live/ dead reagents were added to wells as 0.5 °L calcein AM and 2 °L ethidium homodimer in 1 mL PBS and incubated for 30 min. After 30 min, the reagent was removed, followed by washing the constructs thoroughly with DPBS. Finally, fresh DPBS was added to the constructs to observe the fluorescence emitted by the cells upon excitation of cells at two wavelengths of 494 nm and 528 nm using florescent microscope (Zeiss Axio Observer, Walpole, MA). Live and dead cells were identified according to the color of the stains with red indicates dead and green live cells. We used ImageJ software for stained cell quantification in three different representative sections of each sample.

2.7.3. Cell metabolic activity in oxygen releasing bioink—The effect of O_2 on cellular metabolic activity was measured using colorimetric cell counting kit (CCK-8 assay, Dojindo Molecular Technologies, Rockville, MD, USA). Briefly, 3D printed constructs containing 5×10^6 3T3 cells mL^{-1} or 8×10^6 cardiomyocytes mL^{-1} were cultured in 12 well-plates for 7 days in DMEM with bovine serum and Pen Strep as supplements under hypoxic condition. Three-dimensional constructs were washed with DPBS for three times after each time intervals. Then, 10% CCK-8 reagent in plain medium was added to 3D constructs and incubated for 2h at 37 °C, and changes in color of media from pink to violet were noted. Subsequently, 100 μL of media in each well was transferred into 96 well plates and the absorption of media at 450 nm was measured using the microplate reader (Synergy™ HTX Multi-Mode Microplate Reader, BioTek Winooski, Vermont, USA).

2.8. Statistics

Statistical variations were evaluated using one-way ANOVA in OriginPro software. Bonferroni post-hoc test was used as a comparison test to determine whether there were significant differences. Differences were considered to be statistically significant whenever p was < 0.05, and < 0.01. The mean ± standard deviation (SD) was calculated from 5 replicates of experiments.

3. RESULTS AND DISCUSSION

3.1. Physical Properties of Bioprinted Constructs

In the current study, high degree of functionalization of GelMA (high methacrylated gelatin) was used for the preparation O_2 releasing bioink. Different degrees of methacrylation in GelMA (low, medium, high and very high) can be used in the preparation of bioinks. We did not use very high GelMA, because modification rate decreases the viscosity of bioinks which affects adversely printability [28]. In addition, the presence of CPO can negatively affect the photopolymerization of the bioink. Because of these reasons, we did not consider low and medium GelMA in our study. O_2 releasing bioinks were produced using 10% GelMA, containing CPO in varying concentrations (w/v) of 0.1% (0.1 CPO), 0.5% (0.5 CPO), 1% (1.0 CPO), or 0% (0 CPO) with HEPES-HCl buffer, according to the protocol presented in Table 1 [29]. CPO has a basic pH characteristic; hence, its addition leads to increased pH. To avoid any harmful effect of basic environment, HEPES-HCl buffer was used to adjust pH to 7.0, 7.8 and 8.2 for 0.1, 0.5 and 1% CPO groups of bioinks, respectively, according to the Newland *et al.* [29] (Fig. S1). It should be noted that low pH will enhance O_2 release by increasing H_2O_2 generation rate; accordingly, any excess amount of HCl, that can decrease the pH to lower than 5, should be avoided. It is worth mentioning that the pH values of prepared bioinks were in the range of 6.5–8.5, which are not harmful to cells considering the short printing time (30 min). After printing, constructs were incubated in DMEM cell culture media having pH value of 7.4, which subsequently stabilizes the pH of constructs.

Bioinks were prepared and printed at 4 °C. The effect of CPO on the physical properties of bioinks was evaluated via studying microscopic images of printed constructs, and changes in the spreading ratio of printed fibers were investigated (Fig. 2). The rheological properties

(viscosity measurements) corresponding to different changes in temperature and shear rates were also determined (Fig. 2B). The lowest spreading ratios were obtained from bioinks having 0.5 CPO, as it can be seen in Fig. 2A. This can be explained by the effect of reaching highest viscosity of GelMA bioink at its iso-electric point of 7.8 [30] (Fig. S2). When CPO is added, pH goes up and viscosity increases until reaching the iso-electric point of the GelMA. After passing this point, the viscosity of GelMA goes down. It was noted that bioinks with 0.5% CPO corresponds to the iso-electric point of GelMA. However, with increasing the CPO concentration to 1.0%, the viscosity goes down while pH continues to rise. Accordingly, 0.5 CPO has shown highest viscosity and resulted in the formation of thinner printed fibers (Fig. 2Bi), and on the other hand, 1.0% CPO ink was associated with lowest viscosity and resulted in the formation of the highest spreading fibers (Fig. 2Bi).

Figure 2Bii shows the relationship between bioink viscosity and changes in temperature. It is seen that viscosity significantly decreases with increasing temperatures up to ~20 °C, after which it does not tend to change in the studied range up to 25 °C. Fig. 2Biii shows how the viscosity of bioinks changes with the increasing shear rates. As discussed above, the viscosity significantly affects the printability (Pr) of hydrogels [27]. When the Pr value is close to 1, it shows that bioink can be easily printed. It was found that 0.5 CPO is associated with the highest viscosity, with 0.97±0.01 Pr value which is the closest value to the 1 and accordingly better printing quality and 1 CPO was associated with the lowest viscosity values and with 0.84±0.03 Pr values, which are the farthest from Pr value of 1.

3.2. Morphological Changes and Swelling of 3D Printed O_2 Releasing Constructs

Porosity is one of the most significant characteristics of a biomaterial that needed to be evaluated as it is linked to its swellability. The results of SEM studies that were performed to monitor the effect of incorporated CPO on the morphology and porosity of constructs are shown in Fig. 3. With increased concentration of CPO in the constructs, pore size was increased, which is probably due to released O_2. Furthermore, UV irradiation can be hindered by CPO, and this may result in weaker crosslinking and larger pore size (Fig. 3A). EDX analysis was performed to evaluate the percentage of contained elements (Fig. 3B and S4) and CPO particle dispersion in the printed constructs. As it is seen, with increasing CPO, peaks related to calcium and chloride become larger corresponding to the release $Ca(OH)_2$ and the addition of HCl, respectively.

The effect of CPO on the swelling ratio of O_2 releasing bioinks is presented in Fig. 3C. High O_2 amounts released from 0.5 CPO bioinks indirectly affect the swelling ratio of constructs by inhibiting the photo crosslinking, leading to higher swelling ratios [22, 31]. The swelling ratio of O_2 releasing hydrogels was measured as 10.38 ± 0.29, 11.36± 0.39, 13.68 ± 0.74 and 12.39± 0.64, for 0 CPO, 0.1 CPO, 0.5 CPO and 1.0 CPO, respectively. It was found that the 1% CPO constructs have lower swelling ratio and pore size compared to 0.5% CPO constructs, which corresponds to the highest O_2 releasing rate associated with 0.5 CPO constructs during the first 30 min of bioink preparation, printing and curing (Fig. S3).

3.3. Mechanical Properties of 3D Printed O_2 Releasing Hydrogels

The effect of CPO concentration on the mechanical properties of crosslinked O_2 releasing hydrogels was examined by obtaining stress-strain curve and Young's modulus from the unconfined compression testing at room temperature. Young's modulus of O_2 releasing gels varied with CPO content as shown in Fig. 4. It is seen that increasing CPO content leads to decreased compression modulus of hydrogels. However, O_2 release influences the modulus of the hydrogels. While the highest value of the modulus was obtained from 0% CPO hydrogels, the lowest one was obtained from 0.5 CPO hydrogels. Similar trend was observed with the compression stress and CPO containing hydrogels.

Fig. 4C, shows storage and loss moduli of the hydrogels. Note that angular frequency increases from 0.1 to 10. It can also be seen that storage modulus for all hydrogels is higher than loss modulus, demonstrating elastic behavior of the hydrogels, which enables them to have self-support and preserve their mechanical integrity. Hydrogels without CPO had the highest storage moduli, and this is expected to decrease with the addition of CPO to the hydrogels. The difference between loss and storage moduli decreases with increased CPO content, which demonstrates less elasticity and more stiffness. However, 0.5 CPO hydrogels have higher loss modulus compared to 1.0 CPO hydrogels. Since high amount of CPO is associated with an increase in pH, this will ultimately decrease the storage modulus. Although 0.5 CPO shows lower Young's modulus, 3D bioprinted constructs with 1cm x 1cm dimensions cultured for seven days were mechanically stable and capable of preserving their mechanical and biological integrity. Fig. 1B–E shows a 3D bioprinted construct that preserved its mechanical stability after being passed through pipette tip (Fig. 1B–E) Fig. 1B shows a 5mm x 5mm 3D bioprinted construct. These constructs are mechanically stable even after multiple injections (Fig. 1C–E) (Video 1,2 in supplementary material).

3.4. Oxygen Release Kinetics From CPO-GelMA Hydrogels

The decomposition of CPO to O_2 occurs in two steps. Fist, CPO reacts with water to produce H_2O_2 and $Ca(OH)_2$ leading to increased pH. Secondly, H_2O_2 decomposes to water and O_2 (Eq. 1). Increased pH will affect the H_2O_2 production rate in the hydrogel [32]. Because H_2O_2 can be toxic to cells, catalase was added to make H_2O_2 decomposes to O_2 [33]. As it is seen in Fig. 5, O_2 content of constructs having no CPO is ~0%, while CPO containing printed constructs provided sustained O_2 release for seven days.

$$\begin{aligned} CaO_2(s) + 2H_2O &\rightarrow Ca(OH)_2(s) + H_2O_2 \\ 2H_2O_2 &\rightarrow O_2 + 2H_2O \end{aligned} \qquad \text{(Eq. 1)}$$

At the CPO concentration of 0.5%, pH is lower than CPO with 1% (more CPO is associated with higher pH upon its dissociation). It was previously shown that CPO degrades faster at lower pH, leading to increased amount of released O_2 [34] (Fig. S3). This highest releasing rate increases the porosity while decrease the mechanical properties of 3D printed constructs, as it was discussed in previous sections. Although CPO containing constructs are associated with burst release of O_2, 1 CPO printed constructs release ~30% of O_2 at day 1, ~9% at day 5, and ~4% at day 7 post-printing. In addition, 0.5 CPO and 0.1 CPO constructs release O_2 around 3% and 1% after seven days, respectively. This release profile can be

explained by the fact that CPO rapid reaction rates leads to rapid consumption of loaded CPO capable of generating O_2. Nevertheless, CPO containing printed constructs were able to provide an oxygenated microenvironment for at least seven days.

3.5. Biological Function of The Resulting 3D Constructs

3.5.1. Cell viability—CPO concentrations of 0, 0.1, 0.5 and 1% in GelMA constructs were tested for the assessment of cell viability at four and seven days post-printing. As it can be seen in Fig. 6, increasing the concentration of CPO to 1% had a negative impact on fibroblast viability which might be due to the toxicity resulting from the use of excessive amount of CPO . The addition of CPO up to 0.5 % was found to enhance cell viability both at day 4 and day 7 in hypoxia, which was comparable to that seen normoxia levels. This means that the harmful effects of a hypoxic microenvironment can be prevented by using CPO in GelMA bioink. According to quantification data in Fig. 6b, the difference between the number of live cells in 0.5 CPO and 0 CPO constructs was statistically significant ($p<0.05$ and $p<0.01$).

According to the findings of the present study, the addition of CPO to bioinks can improve cell viability in printed constructs incubated under hypoxic conditions, which can be useful for application in the treatment of ischemic conditions, e.g., following myocardial infarction [8]. This effect on cell viability was observed not only with 3T3 fibroblasts but also with cardiomyocytes. Fig. 7, shows live/dead staining and related cell viability quantification of cardiomyocyte-laden GelMA constructs having either 0% or 0.5% CPO that were incubated under either hypoxic or normoxic conditions for days 3, 5 and 7. Homogenous distribution of living cells in the constructs can be seen throughout the printed structure having 0.5% CPO. There was significantly higher number of living cells in CPO containing constructs as compared to constructs having no CPO, at different time points of 3, 5 and 7 days of incubation. This preservation of cell viability over seven days by using CPO can be related to reduced levels of lactate dehydrogenase levels resulting from decreased number of dead cells [16]. The oxygen-generating properties of CPO-GelMA would not only enhance cell survival by reducing hypoxic stress, but also by reducing necrosis-induced injury to both cells and tissues.

3.5.2. Cell metabolic activity—To assess the metabolic activity of cells, CCK-8 assay was used. However, it should be noted that CCK-8 which is regularly used to assess cellular metabolism, shows only glycolytic nicotinamide adenine dinucleotide (NADH) production, one facet of cell metabolic activity [35]. According to CCK-8 assay, it was found that metabolic activity of 3T3 fibroblasts in 3D bioprinted constructs having no CPO was significantly decreased in hypoxia compared to normoxia (Fig. 8). Upon increasing the CPO concentration in the constructs, cell metabolic activity increased at days 4 and 7. The metabolic activity of cells in constructs having 0.5% CPO in hypoxia was similar to that of cells cultured under normoxic condition. The deference in metabolic activity between constructs having no CPO and those having 0.1 or 0.5 CPO was statistically significant ($p<0.05$ and $p<0.01$, respectively). However, similar to live/dead results, fibroblasts in 3D constructs having 1% CPO had the lowest metabolic activity. These results suggested that CPO in the bioink can provide O_2 rich environment within printed constructs that can help

cells in overcoming ischemic challenge. Similar observation was made with improved metabolic activity of cardiomyocytes in CPO containing 3D printed constructs. The addition of CPO significantly enhanced cardiomyocytes proliferation (Fig. 9), suggesting that CPO can help in improving cell viability and proliferation even when constructs are kept under hypoxic conditions. The incorporation of CPO into the GelMA bioink can eliminate the adverse effects of hypoxic microenvironment for seven days.

Accordingly, the addition of CPO to bioinks and printing of cellular constructs may be a viable option for regenerative therapeutics that ensures the supply of O_2 required for metabolically demanding cells such as cardiomyocytes, especially when oxygen supply is interrupted. Video 3 in supplementary material shows the contractile activity of cardiomyocytes in the 3D printed constructs having 0.5% CPO at day 7 of incubation.

4. CONCLUSIONS

The results of this study demonstrate that 3D bioprinting can be used to develop oxygenated tissue constructs by using calcium peroxide as an O_2 source in the bioink. Optimal concentration of O_2 was found to be associated with the use of 0.5% CPO, since with higher concentrations, cell viability appears to be compromised. Catalase was used to achieve safe conversion of CPO into O_2 and avoiding the release of H_2O_2. With the use of such optimal CPO concentration in fibroblast or cardiomyocyte-laden GelMA printed constructs, cell viability and function can be significantly enhanced when cultured in hypoxic conditions. This study suggests that oxygenated bioinks can be a viable solution to solve current challenges of tissue engineering and tissue regeneration by supplying cells in tissue implants with O_2 before angiogenesis takes place. Oxygen releasing 3D bioprinted constructs developed in this study can significantly benefit regenerative therapeutics. Further *in vivo* results can be useful to demonstrate the effectiveness of such bioprinted constructs using minimally invasive procedures and help the translation of such oxygenated constructs to the clinic.

Supplementary Material

Refer to Web version on PubMed Central for supplementary material.

Acknowledgements

The authors also acknowledge funding from the National Institutes of Health (1R01EB021857 and R01GM126571), American Heart Association Transformational Project Award (18TPA34230036) and TUBITAK-2219 (1059B191700093). V.H. acknowledges Swiss National Foundation Postdoctoral Fellowship (P2EZP2_187980).

References

[1]. Ashammakhi N, Ahadian S, Darabi MA, El Tahchi M, Lee J, Suthiwanich K, Sheikhi A, Dokmeci MR, Oklu R, Khademhosseini A, Minimally Invasive and Regenerative Therapeutics, Advanced Materials, 31 (2019) 1804041.

[2]. Cambria E, Pasqualini FS, Wolint P, Günter J, Steiger J, Bopp A, Hoerstrup SP, Emmert MY, Translational cardiac stem cell therapy: advancing from first-generation to next-generation cell types, npj Regenerative Medicine, 2 (2017) 17. [PubMed: 29302353]

[3]. Kalogeris T, Baines CP, Krenz M, Korthuis RJ, Cell biology of ischemia/reperfusion injury, International review of cell and molecular biology, Elsevier 2012, pp. 229–317.

[4]. Jain RK, Au P, Tam J, Duda DG, Fukumura D, Engineering vascularized tissue, Nat. Biotechnol, 23 (2005) 821–823. [PubMed: 16003365]

[5]. Butt OI, Carruth R, Kutala VK, Kuppusamy P, Moldovan NI, Stimulation of Peri-Implant Vascularization with Bone Marrow-Derived Progenitor Cells: Monitoring by In Vivo EPR Oximetry, Tissue Engineering, 13 (2007) 2053–2061. [PubMed: 17518714]

[6]. Ashammakhi N, Darabi MA, Kehr NS, Erdem A, Hu S.-k., Dokmeci MR, Nasr AS, Khademhosseini A, Advances in Controlled Oxygen Generating Biomaterials for Tissue Engineering and Regenerative Therapy, Biomacromolecules, (2019).

[7]. Hu X, Yu SP, Fraser JL, Lu Z, Ogle ME, Wang J-A, Wei L, Transplantation of hypoxia-preconditioned mesenchymal stem cells improves infarcted heart function via enhanced survival of implanted cells and angiogenesis, The Journal of thoracic and cardiovascular surgery, 135 (2008) 799–808. [PubMed: 18374759]

[8]. Fan Z, Xu Z, Niu H, Gao N, Guan Y, Li C, Dang Y, Cui X, Liu XL, Duan Y, Li H, Zhou X, Lin PH, Ma J, Guan J, An Injectable Oxygen Release System to Augment Cell Survival and Promote Cardiac Repair Following Myocardial Infarction, Sci Rep, 8 (2018) 1371. [PubMed: 29358595]

[9]. Ward CL, Corona BT, Yoo JJ, Harrison BS, Christ G.J.J.P.o., Oxygen generating biomaterials preserve skeletal muscle homeostasis under hypoxic and ischemic conditions, 8 (2013) e72485.

[10]. Steg H, Buizer AT, Woudstra W, Veldhuizen AG, Bulstra SK, Grijpma DW, Kuijer R.J.J.o.M.S.M.i.M., Control of oxygen release from peroxides using polymers, 26 (2015) 207.

[11]. Mallepally RR, Parrish CC, Mc Hugh MA, Ward K.R.J.I.j.o.p., Hydrogen peroxide filled poly (methyl methacrylate) microcapsules: potential oxygen delivery materials, 475 (2014) 130–137.

[12]. Chang CJ, The Effect of Pulse-Released Nerve Growth Factor from Genipin-Crosslinked Gelatin in Schwann Cell-Seeded Polycaprolactone Conduits on Large-Gap Peripheral Nerve Regeneration, Tissue Engineering Part A, 15 (2009) 547–557. [PubMed: 18925830]

[13]. Northup A, Cassidy D, Calcium peroxide (CaO2)for use in modified Fenton chemistry, Journal of Hazardous Materials, 152 (2008) 1164–1170. [PubMed: 17804164]

[14]. Schmidtke T, White D, Woolard C, Oxygen release kinetics from solid phase oxygen in Arctic Alaska, J Hazard Mater, 64 (1999) 157–165. [PubMed: 10337396]

[15]. Clark JM, The toxicity of oxygen, American Review of Respiratory Disease, 110 (1974) 40–50. [PubMed: 4613232]

[16]. Alemdar N, Leijten J, Camci-Unal G, Hjortnaes J, Ribas J, Paul A, Mostafalu P, Gaharwar AK, Qiu YL, Sonkusale S, Liao RL, Khademhosseini A, Oxygen-Generating Photo-Cross-Linkable Hydrogels Support Cardiac Progenitor Cell Survival by Reducing Hypoxia-Induced Necrosis, Acs Biomaterials Science & Engineering, 3 (2017) 1964–1971.

[17]. Alemdar N, Oxygen-Generating Photocrosslinkable Hydrogel, Cell-Based Microarrays, Springer 2018, pp. 241–250.

[18]. Zhang YS, Pi Q, van Genderen AM, Microfluidic bioprinting for engineering vascularized tissues and organoids, JoVE (Journal of Visualized Experiments), (2017) e55957.

[19]. Montgomery M, Ahadian S, Davenport Huyer L, Lo Rito M, Civitarese RA, Vanderlaan RD, Wu J, Reis LA, Momen A, Akbari S, Pahnke A, Li R-K, Caldarone CA, Radisic M, Flexible shape-memory scaffold for minimally invasive delivery of functional tissues, Nature Materials, 16 (2017) 1038. [PubMed: 28805824]

[20]. Wang L, Jiang J, Hua W, Darabi A, Song X, Song C, Zhong W, Xing MMQ, Qiu X, Mussel-Inspired Conductive Cryogel as Cardiac Tissue Patch to Repair Myocardial Infarction by Migration of Conductive Nanoparticles, Advanced Functional Materials, 26 (2016) 4293–4305.

[21]. Shin SR, Zihlmann C, Akbari M, Assawes P, Cheung L, Zhang KZ, Manoharan V, Zhang YS, Yuksekkaya M, Wan KT, Nikkhah M, Dokmeci MR, Tang XW, Khademhosseini A, Reduced Graphene Oxide-GelMA Hybrid Hydrogels as Scaffolds for Cardiac Tissue Engineering, Small, 12 (2016) 3677–3689. [PubMed: 27254107]

[22]. Alemdar N, Leijten J, Camci-Unal G, Hjortnaes J, Ribas J, Paul A, Mostafalu P, Gaharwar AK, Qiu Y, Sonkusale S, Liao R, Khademhosseini A, Oxygen-Generating Photo-Cross-Linkable

Hydrogels Support Cardiac Progenitor Cell Survival by Reducing Hypoxia-Induced Necrosis, ACS Biomaterials Science & Engineering, 3 (2017) 1964–1971.

[23]. Yue K, Trujillo-de Santiago G, Alvarez MM, Tamayol A, Annabi N, Khademhosseini A, Synthesis, properties, and biomedical applications of gelatin methacryloyl (GelMA) hydrogels, Biomaterials, 73 (2015) 254–271. [PubMed: 26414409]

[24]. Ahadian S, Davenport Huyer L, Estili M, Yee B, Smith N, Xu Z, Sun Y, Radisic M, Moldable elastomeric polyester-carbon nanotube scaffolds for cardiac tissue engineering, Acta biomaterialia, 52 (2017) 81–91. [PubMed: 27940161]

[25]. Jia WT, Gungor-Ozkerim PS, Zhang YS, Yue K, Zhu K, Liu WJ, Pi Q, Byambaa B, Dokmeci MR, Shin SR, Khademhosseini A, Direct 3D bioprinting of perfusable vascular constructs using a blend bioink, Biomaterials, 106 (2016) 58–68. [PubMed: 27552316]

[26]. Daly AC, Critchley SE, Rencsok EM, Kelly DJ, A comparison of different bioinks for 3D bioprinting of fibrocartilage and hyaline cartilage, Biofabrication, 8 (2016) 045002.

[27]. Ouyang L, Yao R, Zhao Y, Sun W, Effect of bioink properties on printability and cell viability for 3D bioplotting of embryonic stem cells, Biofabrication, 8 (2016) 035020.

[28]. Lee BH, Lum N, Seow LY, Lim PQ, Tan LP, Synthesis and characterization of types a and b gelatin methacryloyl for bioink applications, Materials, 9 (2016) 797.

[29]. Newland B, Baeger M, Eigel D, Newland H, Werner C, Oxygen-Producing Gellan Gum Hydrogels for Dual Delivery of Either Oxygen or Peroxide with Doxorubicin, ACS Biomaterials Science & Engineering, 3 (2017) 787–792.

[30]. Liang GG, Hawkett BS, Tanner RI, The determination of the isoelectric point from measurements of dispersion viscosity as a function of pH, Journal of dispersion science and technology, 26 (2005) 469–472.

[31]. Hwang CM, Sant S, Masaeli M, Kachouie NN, Zamanian B, Lee S-H, Khademhosseini A, Fabrication of three-dimensional porous cell-laden hydrogel for tissue engineering, Biofabrication, 2 (2010) 035003.

[32]. Nasef A, Ashammakhi N, Fouillard L, Immunomodulatory stromal cells: possible effect of mesenchymal mechanisms, Regen Med, 3 (2008) 531–546. [PubMed: 18588475]

[33]. Abdi SIH, Ng SM, Lim JO, An enzyme-modulated oxygen-producing micro-system for regenerative therapeutics, International journal of pharmaceutics, 409 (2011) 203–205. [PubMed: 21356297]

[34]. https://www.solvay.us/en/binaries/IXPER_Calcium_Peroxide_for_Soil_Amendment-236818.pdf

[35]. Chamchoy K, Pakotiprapha D, Pumirat P, Leartsakulpanich U, Application of WST-8 based colorimetric NAD (P) H detection for quantitative dehydrogenase assays, BMC biochemistry, 20 (2019) 1–14. [PubMed: 30665347]

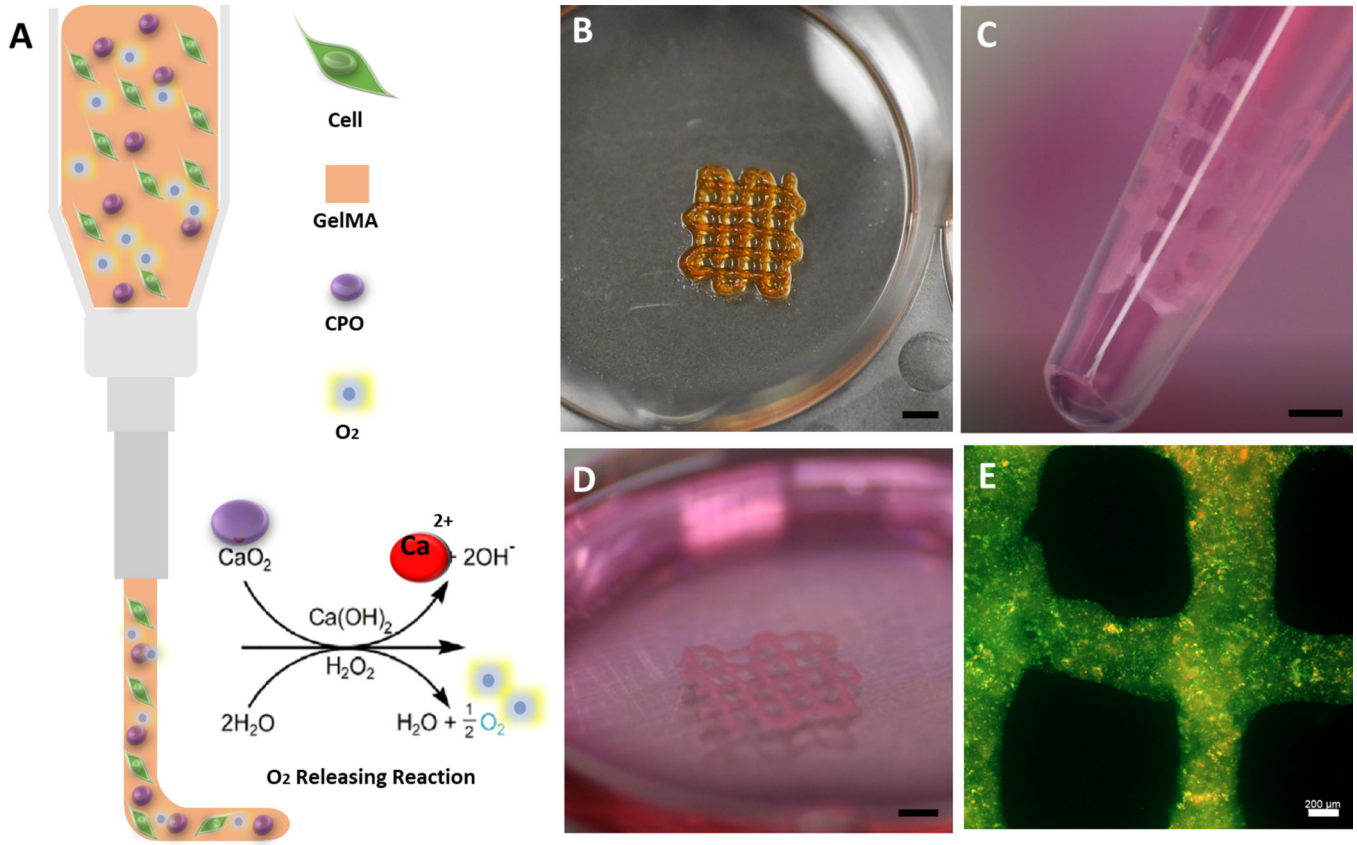

Fig. 1.

Illustration of a 3D bioprinting nozzle, showing cell-laden O_2-releasing bioink and the chemical reaction leading to the formation of O_2. B) Optical image of a 3D bioprinted construct with 0.5 CPO. C) Optical illustration of cardiomyocyte-laden printed construct cultured for 7 days and ready for delivery by injection (orifice diameter: 2.5mm). D) Image of printed construct shown in C after multiple suction and release by injection, which demonstrated its mechanical stability. E) Live/dead staining florescent microscopic image of the printed construct at day 7 after incubation and after injection, demonstrating that cardiomyocytes can survive in the construct even after multiple injection process (Green shows live cells and red shows dead cells) (Scale bars for (B), (C), (D): 2mm; (E): 200 µm).

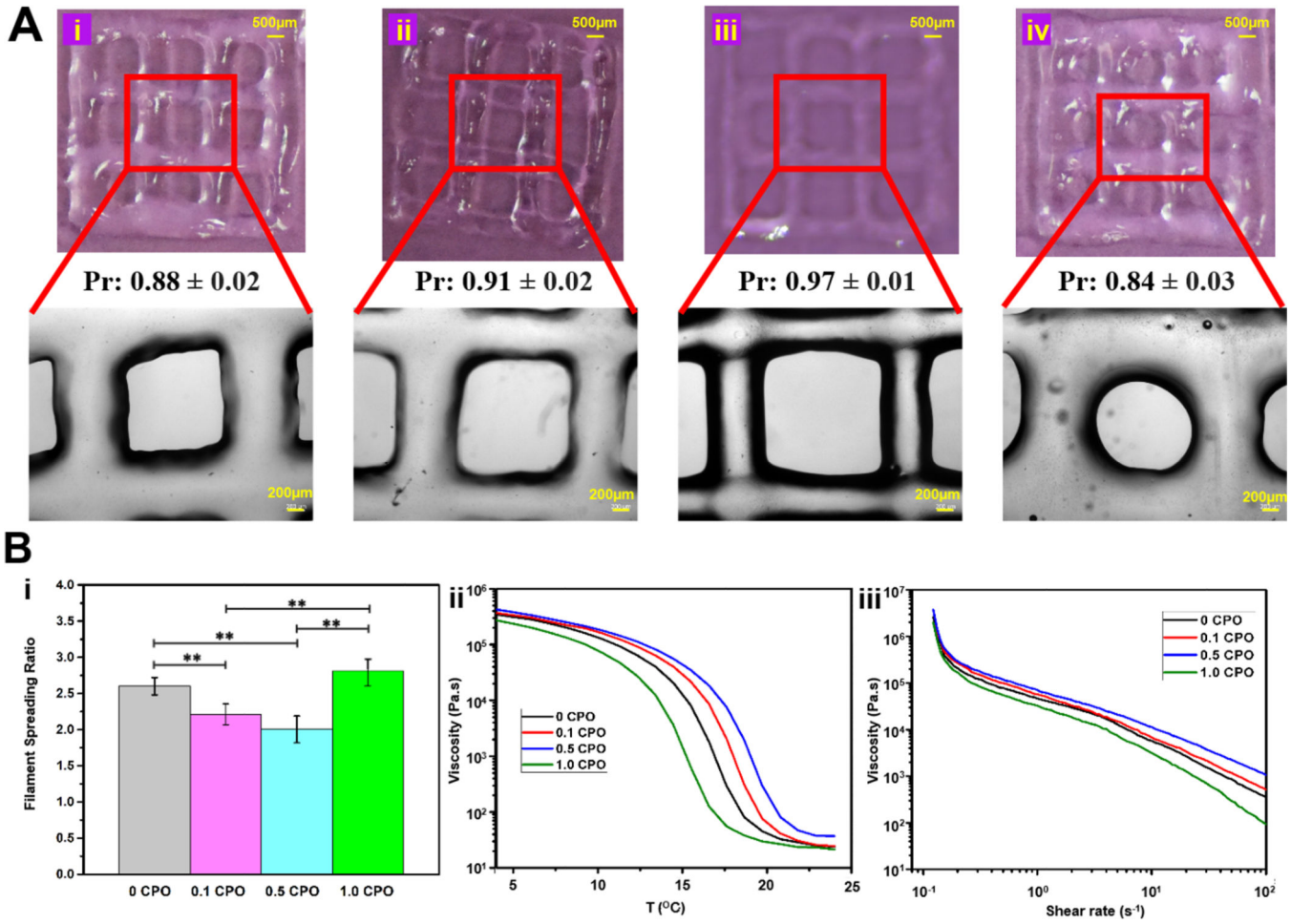

Fig. 2.

A) Images of printed GelMA constructs containing CPO in different concentrations of (i) 0%, (ii) 0.1%, (iii) 0.5% and (iv) 1% with bioink printability values. The second row of microscopic images are magnified locations, that show more closely the morphology of printed meshes. It appears that 0.5% O_2 containing mesh is thinner than others because viscosity is highest among printed constructs. B) Physical properties of printed constructs with varying CPO contents. (i) Effect of viscosity on printed fiber spreading ratio (*, $p<0.05$, significant difference; **, $p<0.01$, significant difference). (ii) Effect of temperature changes on viscosity. (iii) Relation between viscosity and shear rate.

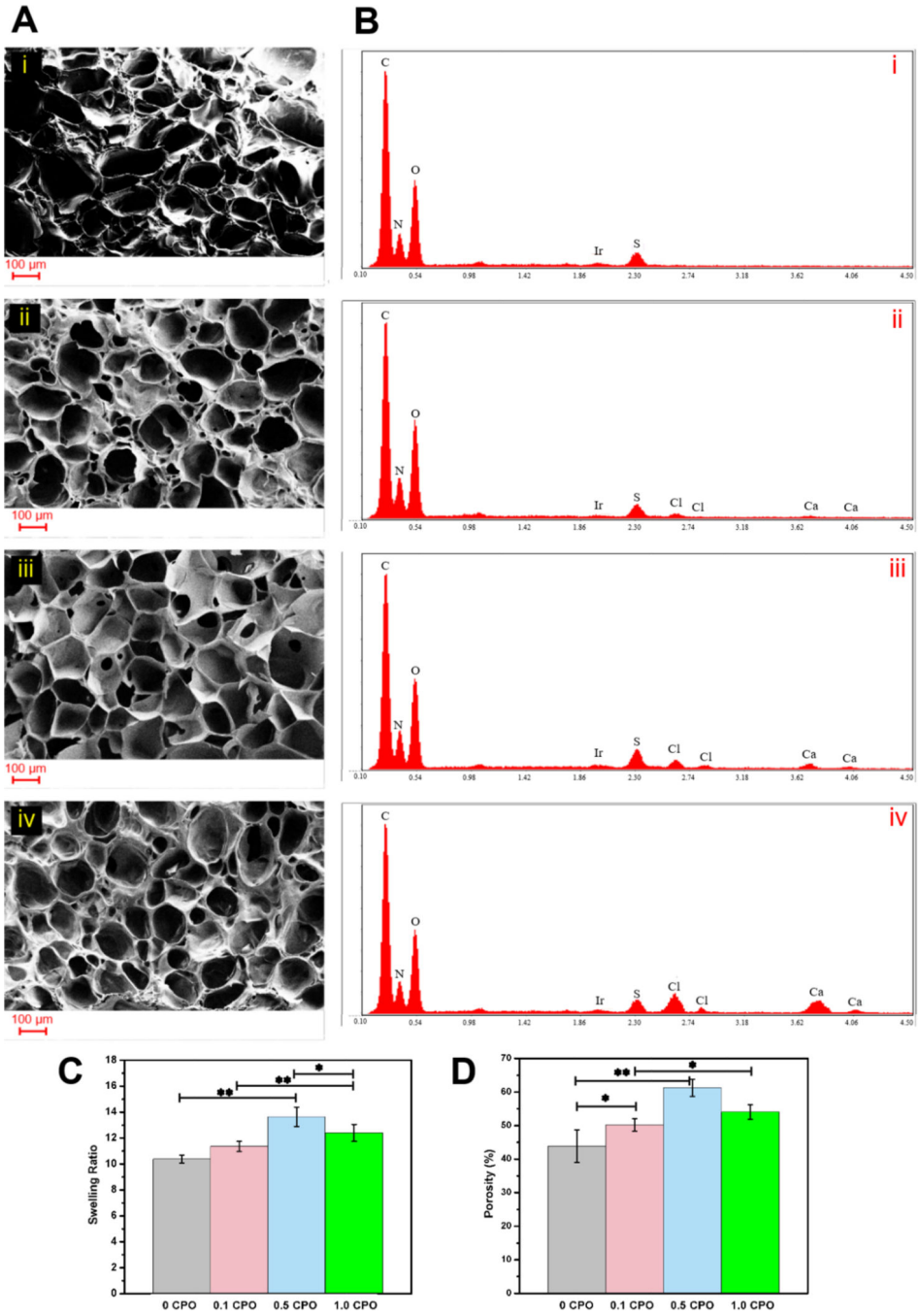

Fig. 3.

Ai-iv) SEM images of GelMA hydrogels containing either 0%, 0.1%, 0.5% or 1% CPO. Note the porous structure of the gels and pore size ranging from 30 to 138 μm. B) (i-iv) EDX evaluation showing the atomic percentage of various elements in the hydrogels. C) Swelling ratio of constructs having different CPO concentrations. D) Semi-quantification of the porosity of hydrogels based on the analysis of SEM images. There was a significant increase in the porosity of gels from 10.2 ± 0.3 % to 13.6 ± 0.7 % when CPO content was increased from 0% CPO to 0.5% (*, $p<0.05$; **, $p<0.01$).

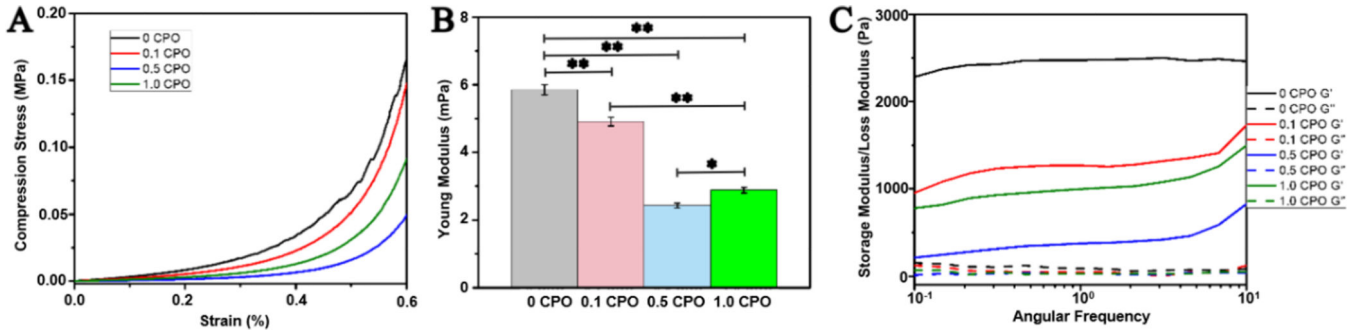

Fig. 4.

Mechanical Properties of GelMA hydrogels containing either 0%, 0.1%, 0.5% or 1% CPO. A) Relation of compressive strength to strain for GelMA hydrogels having different CPO concentrations. B) Young's modulus obtained from compression test (statistically significant difference between samples with and without CPO microparticles can observed, $p<0.05$) C) The storage (G') and loss (G") moduli as a function of frequency (Differences were statistically significant, *, $p<0.05$; **, $p<0.01$).

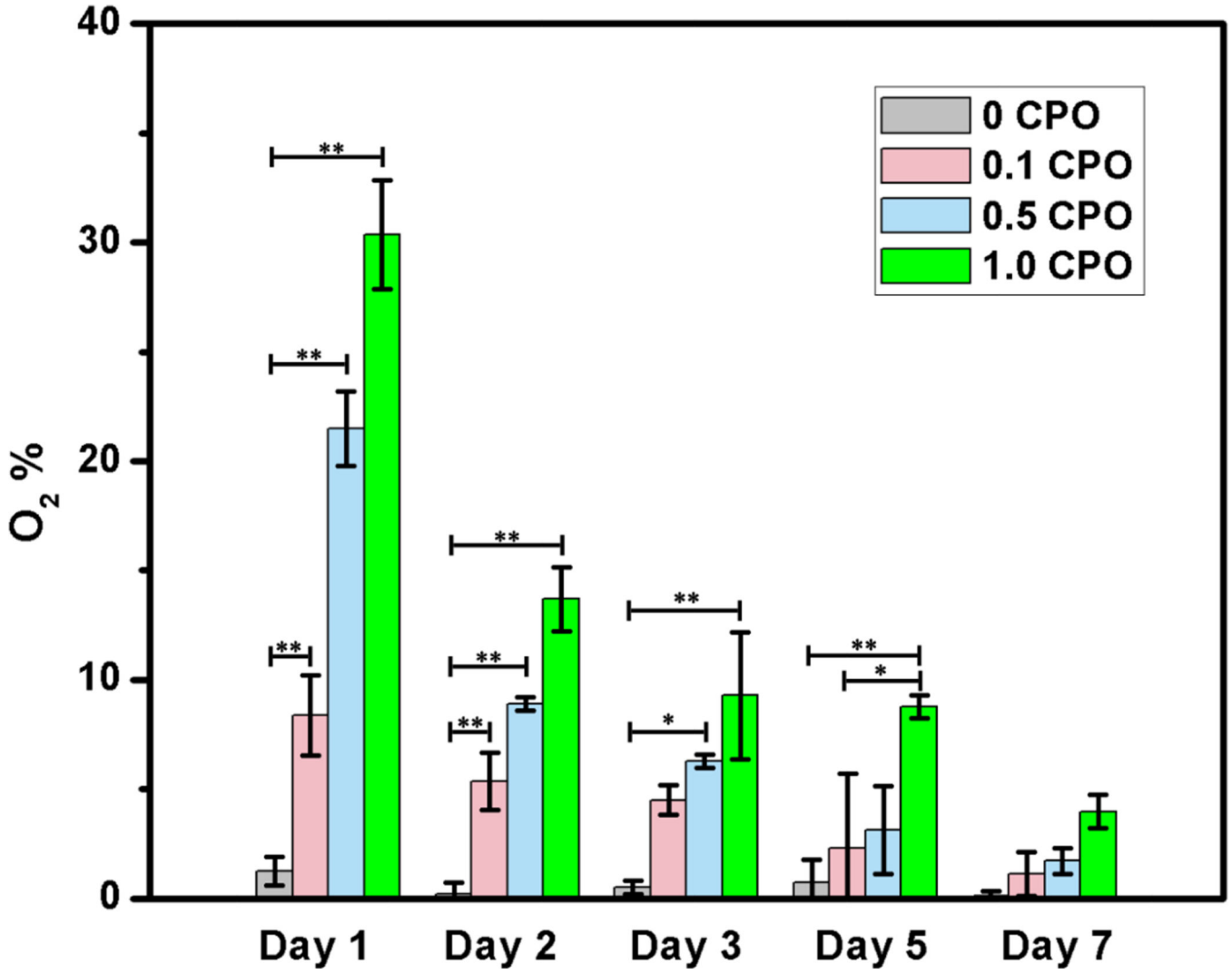

Fig. 5.

O_2 release form CPO laden hydrogels measured daily for seven days, in hypoxic chamber having 1% O_2, 5% CO_2 and 94% N_2. The duration of release continued for seven days (Differences were significant, *, $p<0.05$; **, $p<0.01$).

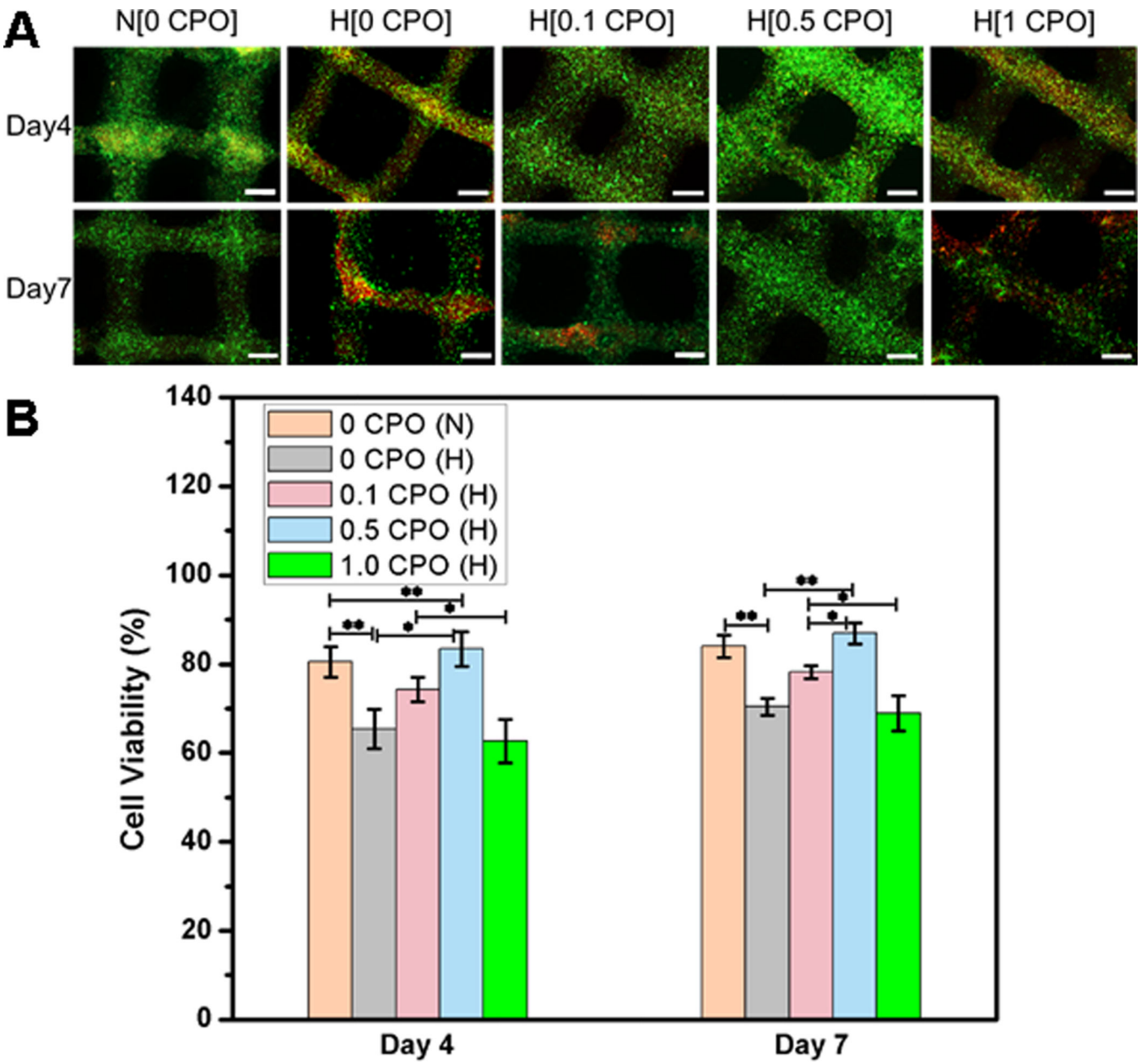

Fig. 6.

A) Live (green)/dead (red) staining of 3T3 fibroblasts printed in GelMA bioinks having different CPO concentrations (0%, 0.1%, 0.5% or 1%). The 3D printed constructs were cultured for seven days either under normoxic (N) (atmospheric oxygen), or hypoxic (H) conditions (1% O_2, 5% CO_2 and 94% N_2). Scale bar denotes 500 °m. B) Quantification of cell viability (statistically significant differences between different constructs was observed, *, $p<0.05$; **, $p<0.01$).

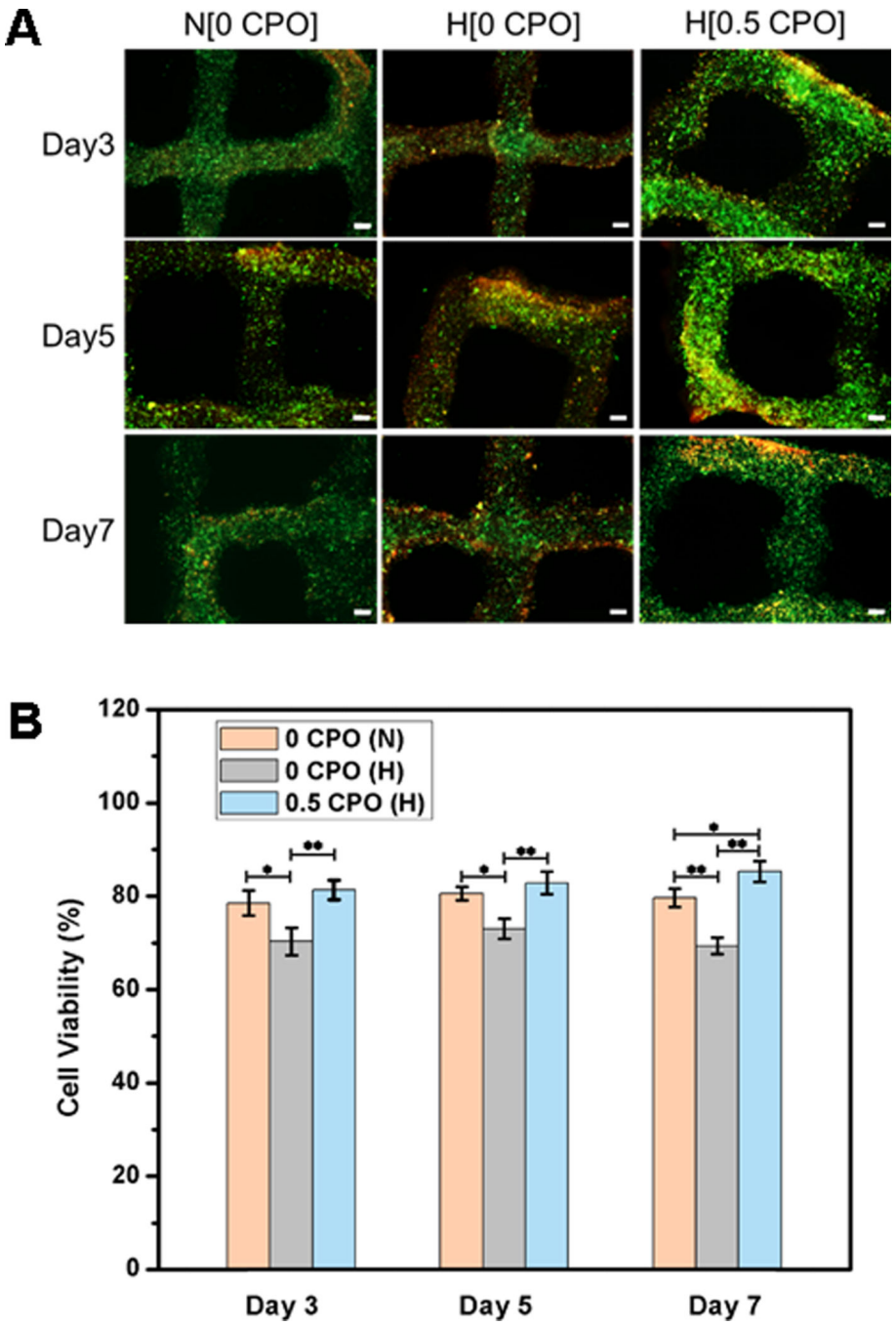

Fig. 7.

A) Live/dead staining of 3D printed cardiomyocyte-laden GelMA constructs having 0% and 0.5% CPO, that were cultured under hypoxic conditions and 0% CPO that were cultured under normoxic condition for three, five and seven days. Scale bar is 200 μm. B) Quantification of cell viability showing significant difference between constructs (*, $p<0.05$; **, $p<0.01$).

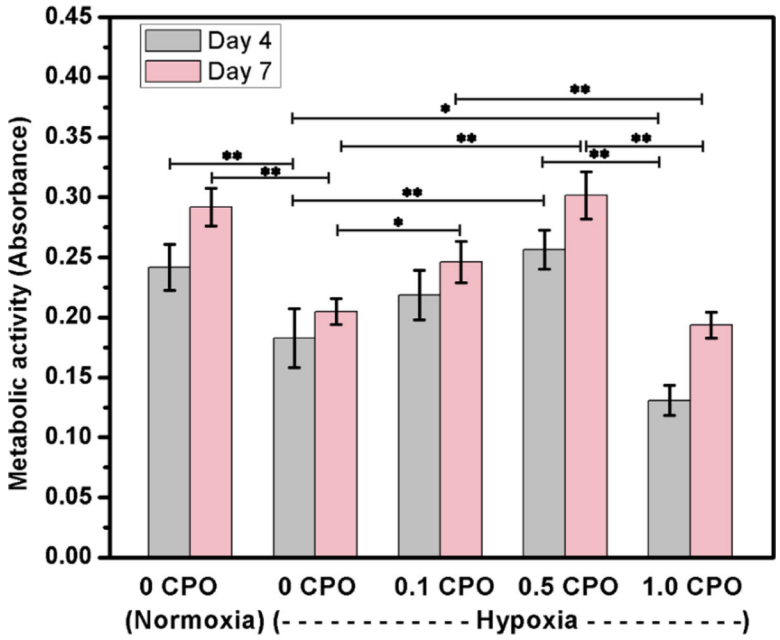

Fig. 8.

Metabolic activity of fibroblasts in 3D printed constructs that contain CPO in different concentrations of 0.1, 0.5 and 1.0%, compared to those that had no CPO, and tested under either hypoxic or normoxic conditions (Statistically significant differences were observed, *, $p<0.05$; **, $p<0.01$).

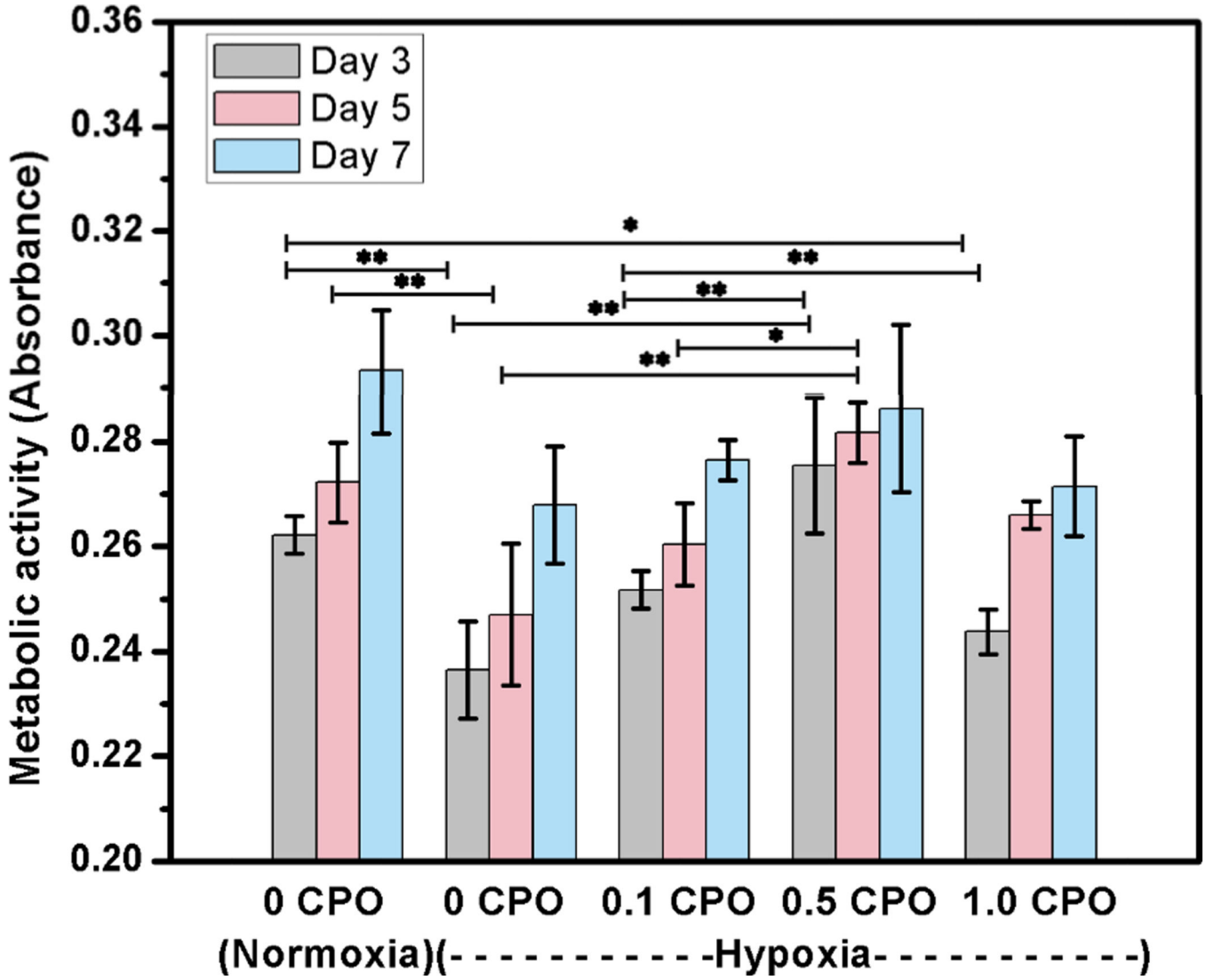

Fig. 9.

Metabolic activity of cardiomyocytes in 3D printed constructs that contain CPO in different concentrations of 0.1, 0.5 and 1.0%, compared to those that had no CPO, and tested under either hypoxic or normoxic conditions (Differences were statistically significant, *, $p<0.05$; **, $p<0.01$).

Table 1.

Production of O_2 generating bioinks with varying CPO content.

Bioinks	GelMA solution volume (20% GelMA + 1% PI in HEPES)	CPO solution volume (2% CPO in HEPES+ HCL)	HEPES volume
0 CPO	0.5 mL	-	0.5 mL
0.1 CPO	0.5 mL	0.05 mL	0.45 mL
0.5 CPO	0.5 mL	0.25 mL	0.25 mL
1.0 CPO	0.5 mL	0.5 mL	-